

## Iron Based Nano-hydrotalcites Promoted with Cu as Catalysts for Fischer-Tropsch Synthesis in biomass to Liquid Process

Arian Grainca<sup>b</sup>, Alessandro Di Michele<sup>a,c</sup>, Claudio Sugliani<sup>b</sup>, Elisa Boccalon<sup>d</sup>, Morena Nocchetti<sup>a,e</sup>, Claudia Bianchi<sup>a,b</sup>, Carlo Pirola<sup>a,b\*</sup>

<sup>a</sup>National Interuniversity Consortium of Materials Science and Technology (INSTM), Florence, Italy

<sup>b</sup>Università degli Studi di Milano, Dipartimento di Chimica, Milano (Italy)

<sup>c</sup>Università di Perugia, Dipartimento di Fisica e Geologia, Perugia (Italy)

<sup>d</sup>Università di Salerno, Dipartimento di Ingegneria Industriale, Fisciano, SA (Italy)

<sup>e</sup>Università di Perugia, Dipartimento di Scienze Farmaceutiche, Perugia (Italy)

arian.grainca@unimi.it

Two different groups of MgCuFe catalysts derived from hydrotalcite-like precursors were prepared through ultrasound-assisted (US) co-precipitation and solvent-free ball milling methods (BM). The catalysts were activated at 623°K, 1.5 MPa for 4 h in syngas, and their performances in the production of fuels through Fischer–Tropsch (FT) synthesis were evaluated in a fixed bed reactor at temperatures ranging from 473° to 573°K and 2 MPa and H<sub>2</sub>/CO molar ratio of 2. The physicochemical properties of the fresh and spent catalysts were investigated and characterized using different methods, including XRPD, ICP-OES, SEM, and TEM. Catalysts displayed similar catalytic activity for both BM and US with minor differences when operating at temperatures from 473° to 523°K. The results hint at the possibility of using synthetic hydrotalcites as Fe-based catalysts for the Fischer–Tropsch synthesis.

### 1. Introduction

The dramatic increase in the worldwide population and industrial/daily activities has led to the huge consumption of fuels and chemical products. On a large scale, from one side, the production of fuels to satisfy the human need is still challenging, especially in the following decades, as more activities and increase in the population are expected. On the other hand, many real-world processes to produce fuels may lead to secondary pollution or/and are not appropriate production of required amounts. In this sense, the scientific community has given much attention nowadays to the possibility of hydrocarbon production from renewable resources as environmentally friendly and economical processes (Olusola O. James, 2012). One common synthesis approach at an industrial scale is Fischer–Tropsch synthesis (FTS), which is widely used to produce fuels and worthy valuable chemicals (e.g., methanol, ethanol, and olefins). Typically, Fischer-Tropsch fuels are produced from coal and natural gas (CTL, GTL) rather than biomass (BTL) (Nima Mirzaeia, 2021) since both the economic feasibility of small-scale plants and government limitations to the accumulation of biomass are to be met in order to render the process performable (Chelsea L. Tucker, 2020). For economic, environmental, and sustainable reasons, many research groups nowadays are developing FTS-based approaches for the green production of fuels from alternative sources rather than coal and natural gas. FTS has been commercially adopted for many years and is still alluring much attention for transportation fuel production due to the variety of raw materials used (Hadhadev-Kostic M, 2011; Tingjun Fu, 2013). The essential target of FTS relies on the production of paraffins and olefins with varying molecular weights whilst limiting the formation of methane and carbon dioxide. (Zhang Qinghong, 2010). FTS usually requires catalysts based on iron or cobalt. Loads of synthesis methods that combine different transition metals (including Ni, Ru, Fe, and Co) have been developed over the last decades (F. Pardo-Tarifa, 2017; X. Zhao, 2018). Iron and cobalt-based catalysts produce less methane than Ni making them more appealing, while Ru is prohibitive for its renowned high cost.

Iron catalysts are often preferred over cobalt-based ones, especially when converting syngas with a molar  $H_2/CO$  ratio lower than 2, which is also the typical ratio of syngas coming from biomass or coal (Torres Galvis, 2013). On the other hand, when feeding a syngas mixture with an  $H_2/CO$  ratio close to 2, cobalt catalysts are preferred due to their high selectivity towards heavy hydrocarbons and their low activity in WGS reaction limiting the  $CO_2$  formation.

In this work, we propose double- and triple-layered hydroxides, also known as hydrotalcite-like compounds (HTlc), as a novel catalyst for the FT process. In fact, especially for iron-based hydrotalcite, there is a lack of studies in the literature. HTlc basically consists of mixed metal hydroxides, where specific metal atoms are homogeneously dispersed at an atomic level. HTlc are represented by the formula  $[M(II)_{1-x}M(III)_x(OH)_2]^{x+}[A_n]^{x-}mH_2O$  where  $M(II)$  is a divalent cation such as Co, Mg, Zn, Ni, or Cu,  $M(III)$  is a trivalent cation such as Al, Cr, Fe or Ga;  $A_n$  is an anion of charge  $n$  and  $m$  the molar amount of co-intercalated water. If calcined at appropriate temperatures, the random distribution of cations, characteristic of the hydroxide phase, is maintained in the resulting mixed oxide. HTlc-based materials have been recently reported as suitable catalysts for several processes in the energy field, such as transesterification and biodiesel production (Renata A.B. Lima-Correa, 2020), steam reforming of ethanol for hydrogen production (Doris Homsí, 2016), and methane reforming (M.E.Rivasa, 2008). Recently, a series of studies on Co-based hydrotalcites were performed (Angélica Forgianny, 2016) especially taking into account the use of HTlc as support of the FTS catalyst (Jae-Sun Jung, 2016) in which the catalytically active metal is dispersed on the HTlc surface (Yu-Tung Tsai, 2011). Moreover, both the techniques involved in this work's synthesis, ultrasound and ball milling, were studied lately for a series of different catalysts active towards  $CO_2$  reduction, conferring substantial improvements in areas such as: high dispersion of active sites, control of particle dimensions, and enhanced catalyst stability (Maela Manzoli, 2018). In the present paper, a new kind of FTS catalyst, in which the active metal is part of the structural core of the HTlc, has been synthesized and tested.

A series of MgCuFe hydrotalcites, with two preparation methods (ball milling and ultrasound), were synthesized both by ultrasound-assisted co-precipitation method and solvent-free mechanochemical technique, characterized and compared in such class of catalyst production. In this study,  $SiO_2$  was used as support since its presence results in more significant activity, especially for Fe-based catalysts (Fangxu Lu, 2021). Activity tests conducted in a packed bed continuous reactor confirmed the catalytic activity. Moreover, these materials' structural and catalytic properties were verified under FTS operating conditions, and correlations between catalyst features and efficiency towards light and heavy hydrocarbons selectivities were achieved.

## 2. Experimental part

### 2.1 Catalyst synthesis

The sample MgCuFe-US was synthesized by means of an ultrasound-assisted co-precipitation method. Specifically, 50 mL of NaOH 1M and  $NaHCO_3$  2M solution was added dropwise to 56 mL of nitrate salts of Mg, Fe, and Cu 1 M solution (molar ratio  $Mg/Fe/Cu=13.2/6/1$ ). During the addition process, the solutions were sonicated with ultrasounds (20 kHz) for 3.5 min, and the sample was maintained at 278°K. A yellow-brown solid precipitated immediately. 100 mL of distilled water was added to dilute the precipitate when the addition was complete. The solid was recovered by centrifugation and repeatedly washed with deionized water, then dried in an oven at 333°K. The final composition, determined by ICP-OES, of MgCuFe-US is:  $[Mg_{0.67}Cu_{0.045}Fe_{0.29}(OH)_2](CO_3)_{0.15} 0.5 H_2O$ .

MgCuFe-BM was synthesized with a solvent-free method by mixing the salts with a proper amount of NaOH in pellets. To prepare 1 g of catalyst 1.96 g of  $Mg(NO_3)_2 \cdot 6H_2O$ , 0.14 g of  $Cu(NO_3)_2 \cdot 3H_2O$ , 1.34 g of  $Fe(NO_3)_3 \cdot 9H_2O$  and 0.888 g of NaOH (molar ratio  $Mg/NaOH = 3/1$ ; molar ratio  $Mg/Fe/Cu=13.2/6/1$ ) reagents were milled for 30 minutes at a frequency of 30 Hz in a planetary mill (Retsch MM200 swing mill, capacity 10 mL, provided with zirconia balls with diameters 10 mm). The solid was collected and transferred in a Teflon bottle filled with 50 mL of distilled water. The precipitate was aged in an oven at 353°K for 3 days. The solid was recovered by centrifugation, washed three times with deionized water and dried at 333°K. The MgCuFe-US composition, obtained by ICP-OES measurements, is:  $[Mg_{0.67}Cu_{0.045}Fe_{0.29}(OH)_2](CO_3)_{0.15} 0.5 H_2O$ . The two hydrotalcites were soaked for 2 h in a  $KNO_3$  solution ( $K \text{ wt}\%=0.5\%$ ),  $T=353^\circ K$ .

### 2.2 Characterization Techniques

XRD patterns of powdered samples were collected with a X'PERT PRO diffractometer (PanAlytical, Roiston, UK) operating at 40 kV and 40 mA equipped with a X'Celerator detector. Measurements were recorded in the 3-70(°)  $2\theta$  range with a 0.030°  $2\theta$  step size and 30 s step scan. The metal content of samples was determined by inductively coupled plasma optical emission (ICP-OES) spectrometer 700-ES series (Varian, Santa Clara, CA, USA). 5 mg of each sample was dissolved in concentrated  $HNO_3$ , and distilled water was added to a total

volume of 100 mL. The morphology of the samples was analyzed by field emission scanning electron microscopy FE SEM LEO 1525 (ZEISS). The sample was deposited on aluminum support using conductive carbon adhesive tape. Before the analysis, the samples were metalized with a thin layer of chromium (8 nm). Measurements were carried out using an In-lens detector at 15 kV. Elemental composition and chemical mapping were determined using a Bruker Quantax EDX. TEM images were obtained using a Philips 208 Transmission Electron Microscope. The samples were prepared by putting one drop of an ethanol dispersion of the catalyst powder on a copper grid pre-coated with a Formvar film and dried in air.

### 2.3 Fischer-Tropsch bench-scale reactor

Three mass flow controllers (Brooks) metered H<sub>2</sub> (32 Nml min<sup>-1</sup> 99.9% purity), CO (16 Nml min<sup>-1</sup>, 99.9% purity) and N<sub>2</sub> (internal standard, 5 Nml min<sup>-1</sup>, 99.99% purity) in a continuous mixer. The mixture entered from the top of a 6 mm internal diameter packed bed reactor charged with 1 g of fresh catalyst mixed with 0.5g of SiO<sub>2</sub>, as diluting material as it confers an improvement in the loss of heat (Fangxu Lu, 2021). A blank test assured that its internal surface was inactive while the catalyst bed was held in place by two pieces of quartz wool. A furnace heated the reactor, and its temperature was monitored with a K-type thermocouple. A second K-type thermocouple monitored the reactor's internal temperature. The catalyst activation was performed at 623°K and 0.4 MPa for 4 hours with the same flow of reagents (total of 53 Nml min<sup>-1</sup>) with CO/H<sub>2</sub> or pure H<sub>2</sub>. Liquid products (water and C<sub>7+</sub>) were condensed in a 0.13 L cold trap with an external cooling jacket at 278°K and subsequently analyzed by gas chromatography. The pressure was maintained at 2.0 MPa with a pneumatic back pressure regulator. Permanent gases and non-condensable hydrocarbons passed through another condenser and were analyzed by an Agilent 3000A micro gas chromatograph, to determine CO conversion ( $X_{CO}$ ) based on N<sub>2</sub> and CO peak areas ( $A_{N_2}$ , and  $A_{CO}$ ), their relative response factor ( $k$ ), and inlet (set) flowrate of N<sub>2</sub> and CO ( $F_{in, N_2}$ , and  $F_{in, CO}$ ) (Eq.1).

$$X_{CO} = \frac{F_{in, CO} - F_{in, N_2}}{F_{in, CO}} \times k \frac{A_{CO}}{A_{N_2}} \quad (1)$$

The instrument, mounted with molsieve and QPLOT columns, sampled the effluent every 2 hours. A mass molar balance was performed for each FT run, resulting in a maximum error of ±5% on a molar basis. The characterization analyses were performed on the catalyst before and after the activation procedure performed in situ in the reactor. "Fresh catalysts" indicates the samples as prepared before activation. "Activated catalysts" indicate the samples activated in the FTS reactor by the reduction activation procedure and removed from the reactor.

## 3. Results and discussion

### 3.1 Characterization

SEM and TEM images of the MgCuFe-US and MgCuFe-BM samples are shown in Figure 1. In both cases, the crystals appear flat and hexagonal. The platelet size distribution is not homogeneous; the samples are characterized by platelets in the 50-80 nm and 40-100 nm range for MgCuFe-US and MgCuFe-BM, respectively. Small crystals are more common in MgCuFe-BM, and the type of synthesis also affects the crystallinity, which is reduced in the sample prepared by the ball mill, so aging treatment is required in this case.

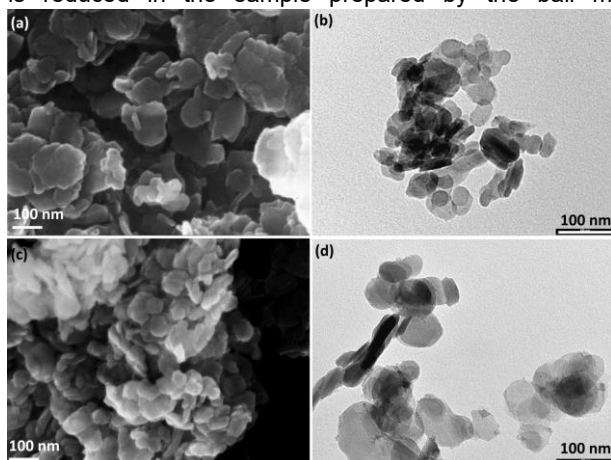


Figure 1: SEM and TEM images of MgCuFe-US (a and b) and MgCuFe-BM (c and d).

An indication of the different degrees of crystallinity is better shown by comparing the XRD patterns of the samples. The XRD patterns of the two samples are reported in Figure 2. In both cases, the interlayer space of HTlc hosts carbonate ions, as indicated by the position of the first reflection at  $2\theta = 11.7^\circ$ . The comparison of the spectra of MgCuFe-BM before and after the thermal treatment indicates that the as-synthesized sample is rather amorphous: the peaks are broad, and the (110) and (113) diffraction planes are not clearly distinguished, appearing as a single reflection peak. Even after the aging process, the intensities of the sample are not comparable with those of MgCuFe-US, confirming the presence of particles of reduced crystallinity and small dimension. Note, in the MgCuFe-US pattern, a peak at  $2\theta = 32.3^\circ$ , highlighted with an asterisk, is probably due to a residue of Na-containing compound.

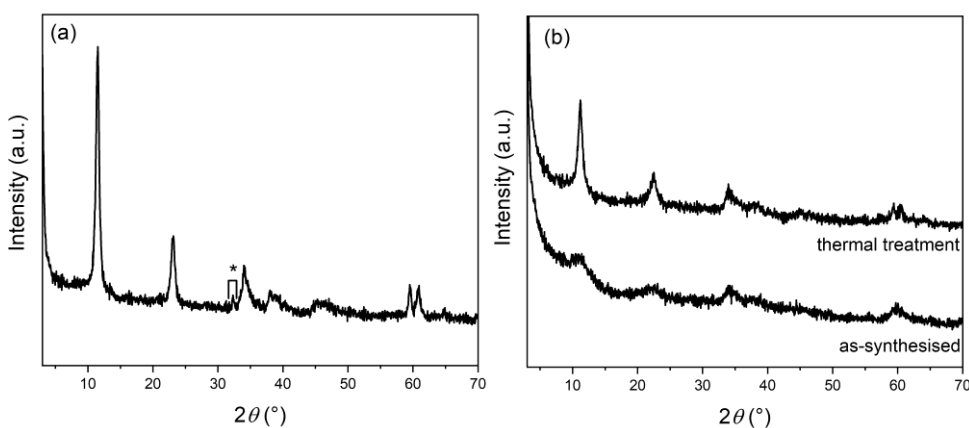


Figure 2: XRD of MgCuFe-US (a) and MgCuFe-BM (b).

### 3.2 FT results

We evaluated the selectivity to methane, CO<sub>2</sub>, light hydrocarbons (C<sub>2-6</sub>, i.e., with a carbon number from 2 to 6), and longer chain hydrocarbons (C<sub>7+</sub>, i.e., with more than 6 carbon atoms). Post-activation characterization allowed us to evaluate the different impacts of the activation by H<sub>2</sub>/CO mixture or by pure hydrogen. Considering the better results (not reported in this paper for space reasons) obtained by activating in syngas flow, only the so activated samples were tested at temperatures ranging from 473 to 573 °K. The FT reactor took 14 h to reach -state conditions, i.e., flow and compositions constant vs. reaction time. Here, we report data collected after this start-up period. The furnace ramped the temperature to 473°K and held it for just over 18 h, It then ramped the temperature to 493 °K and held it for another 24 h and replicating the same procedure for 523°K, 543°K and 573°K (figure 2).

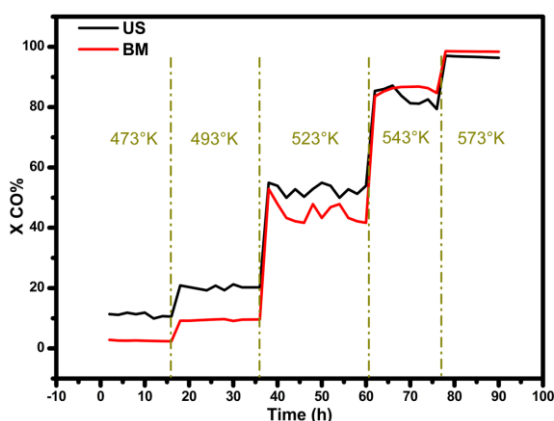


Figure 3: CO conversion of both MgCuFe-US (blue) and MgCuFe-BM (red) hydrotalcites at different temperatures.

The FTS results reported in Figure 3 and Table 1 demonstrated that this kind of catalyst, where iron is incorporated into the HTlc structure rather than supported on the HTlc, is without doubt active for this synthesis. This conclusion is not obvious. In fact, in the typical HTlc structure, iron is ideally present as individual iron ions;

this catalytic structure is very different from those of the commonly used iron supported catalyst for FTS where Fe is present in metallic form (A. E. Kuz'min, 2005)

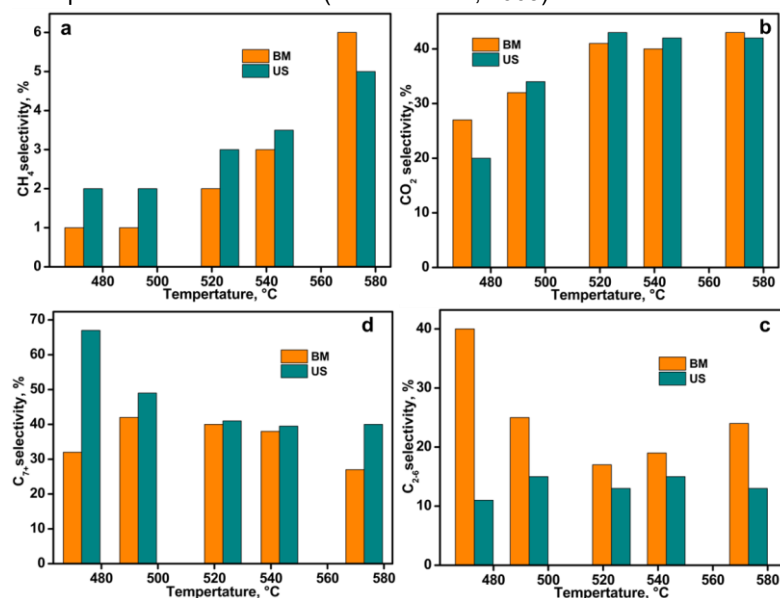


Figure 4: Selectivity towards FTS products; a) CO<sub>2</sub> selectivity, b) CH<sub>4</sub> selectivity, c) C<sub>2-6</sub> fraction selectivity d) C<sub>7+</sub> fraction selectivity.

As expected, for both catalysts, the activity is influenced by the reaction temperature: the higher the temperature, the higher the CO conversion, but also the selectivity towards CO<sub>2</sub>, CH<sub>4</sub>, and light hydrocarbons is favored by a higher temperature. As can be seen by the trends of both US and BM, at 573 K, the conversion reached is maximum (Table 1), while slight differences in activity are manifested at lower temperatures, indicating that at 473°-493°-523°C, the US sample shows CO conversion about 10% higher respect the corresponding ones obtained with BM HTLc.

Table 1: Overall conversion and selectivity results

Sample	Temperature (°K)	Product selectivity %				CO conv %	C <sub>2+</sub> yield
		CH <sub>4</sub>	CO <sub>2</sub>	C <sub>2-6</sub>	C <sub>7+</sub>		
MgCuFe BM	473	1	27	40	32	2.6	1.8
	493	1	32	25	42	9.5	6.4
	523	2	41	17	40	43.3	24.7
	543	3	40	19	38	86.3	49.2
	573	6	43	24	27	98.5	50.2
MgCuFe US	473	2	20	11	67	11.2	8.7
	493	2	34	15	49	20.2	12.9
	523	3	43	13	41	52.8	28.5
	543	4	42	15	40	83.2	45.3
	573	5	42	13	40	96.7	51.3

The selectivity towards CO<sub>2</sub> and CH<sub>4</sub> shows a similar incremental tendency for both catalysts, as visible in Figure 4. Significant diversity is manifested regarding the C<sub>2-6</sub> and C<sub>7+</sub> where incrementing the temperatures, the Fe-based BM shows higher yield in C<sub>2-6</sub> in respect to the US, whereas the latter displays higher selectivity towards the C<sub>7+</sub> fraction. Bearing in mind that the overall C<sub>2+</sub> yield has similar values goes to show that, despite the similar conversion manifested, ball milling and ultrasound iron-based hydrotalcites show different selectivity in terms of short or long hydrocarbon chain production. The efficiency of the catalysts was compared with studies on other iron-based presents in the literature, demonstrating higher catalytic activity with respect to classical silica-supported iron catalysts as FeSi or FeSBA-15, while a slight underperformance when challenging the activity of costly iron-based metallosilicates as Fe/Ce/SiO<sub>2</sub> and Fe/Zr/SiO<sub>2</sub>. For example, the conversion of

Fe<sub>15</sub>Si catalyst was 50%, at 553°K and 1.5MPa, with selectivity towards C<sub>7</sub>+ under 40% (Chike George Okoye-Chine, 2021) while previously mentioned metallosilicates show conversion in ranges of 50 to 60%, at 523°K and 2.0MPa, with selectivity towards the heavy phase of 55 to 65% (Tugce N. Eran, 2022).

#### 4. Conclusions

New Fe-based hydrotalcite-like compounds were synthesized and used as catalysts in the Fischer–Tropsch synthesis. Two different synthetic pathways of Fe-based catalysts and different reaction temperatures were thoroughly investigated. As expected, the catalytic activity of the samples rigorously depends on the temperature. The goal of this study was the evaluation of applying this new kind of catalysts in the Fischer–Tropsch synthesis and the comparison of the two preparation techniques (ball milling and ultrasound), which resulted in similar ability in CO conversion at higher temperatures. In contrast, under 523°K, Fe-based US proved better catalytic activity by 10%. As overall consideration, the tests performed at 573 K provide 50,2% for ball milling and 51,3% for ultrasound in C<sub>2</sub>+ yield and conversions up to 98.5% which are the highest among the reaction ran at different temperature. Since the gathered results were promising, further studies on HTLc as catalytic materials are to be pursued. The subsequent research will involve investigating the effects of different parameters, such as morphology and size of crystallites and the use of this catalyst in CO<sub>2</sub> hydrogenation.

#### References

- A. E. Kuz'min, Y. N. (2005). Fischer-Tropsch Catalysts Based on Zr-Fe Intermetallides Encapsulated in an Al<sub>2</sub>O<sub>3</sub>/Al Matrix. *Kinetics and Catalysis*, 743-751.
- Angélica Forgiionny, J. L. (2016). Effect of Mg/Al Ratio on Catalytic Behavior of Fischer–Tropsch Cobalt-Based Catalysts Obtained from Hydrotalcites Precursors. *Topics in catalysis*, 230-240.
- Chelsea L. Tucker, E. S. (2020). Activity and selectivity of a cobalt-based Fischer-Tropsch catalyst operating at high conversion for once-through biomass-to-liquid operation. *Catalysis today*, 115-123.
- Chike George Okoye-Chine, M. M. (2021). Fischer–Tropsch synthesis: The effect of hydrophobicity on silica-supported iron catalysts. *Journal of Industrial and Engineering Chemistry*, 426-433.
- Doris Homsí, J. A. (2016). Steam reforming of ethanol for hydrogen production. *PROCESS ENGINEERING FOR POLLUTION CONTROL AND WASTE MINIMIZATION*.
- F. Pardo-Tarifa, S. C.-D. (2017). Ce-promoted co/al<sub>2</sub>o<sub>3</sub> catalysts for fischer–tropsch synthesis. *International Journal of Hydrogen Energy*, 9754–9765.
- Fangxu Lu, X. C. (2021). Revealing the activity of different iron carbides for Fischer-Tropsch. *Applied Catalysis B: Environmental*.
- Hadnadev-Kostic M, T. J.-N. (2011). B. Mg–Fe-mixed oxides derived from layered double hydroxides: a study of the surface properties. *J Serb Chem Soc*, 76(12):1661–71.
- Jae-Sun Jung, a. G.-H. (2016). Effect of cobalt supported on meso–macro porous hydrotalcite in Fischer–Tropsch synthesis. *RSC Advances*.
- M.E.Rivasa, J. R.-L. (2008). Preparation and characterization of nickel-based mixed-oxides and their performance for catalytic methane decomposition. *catalysis today*, 367-373.
- Maela Manzoli, B. B. (2018). Microwave, Ultrasound, and Mechanochemistry: Unconventional Tools that Are Used to Obtain "Smart" Catalysts for CO<sub>2</sub> Hydrogenation. *Catalysts*.
- Nima Mirzaeia, A. T. (2021). Flexible Production of Liquid Biofuels via Thermochemical Treatment of Biomass and Olefins Oligomerization: a Process Study. *CEt CHEMICAL ENGINEERING TRANSACTIONS*, 187-192.
- Olusola O. James, B. C. (2012). Reflections on the chemistry of the Fischer–Tropsch synthesis. *RSC Advances*, 7347-7366.
- Renata A.B. Lima-Correa, C. S. (2020). The enhanced activity of base metal modified MgAl mixed oxides from. *Renewable energy*, 1984-1990.
- Tingjun Fu, Y. J. (2013). Effect of carbon support on Fischer–Tropsch synthesis activity and product distribution over Co-based catalysts. *Fuel Processing Technology*, Pages 141-149.
- Torres Galvis, H. M. (2013). Catalysts for Production of Lower Olefins from Synthesis Gas: A Review. *American Chemical Society*, 2130–2149.
- Tugce N. Eran, F. G. (2022). Metallosilicates as an iron support to catalyze Fischer-Tropsch synthesis. *Catalysis Today*.
- Zhao X., S. L. (2018). Comparison of preparation methods of iron-based catalysts for enhancing fischer-tropsch synthesis performance. *Molecular Catalysis*, 99–105.
- Yu-Tung Tsai, X. M. (2011). Hydrotalcite supported Co catalysts for CO hydrogenation. *Applied Catalysis A*, 91-100.
- Zhang Qinghong, K. J. (2010). Development of Novel Catalysts for Fischer–Tropsch Synthesis: Tuning the Product Selectivity. *ChemCatChem*.